2023 IEEE International Conference on Robotics and Automation (ICRA 2023)
May 29 - June 2, 2023. London, UK

Holistic view of Inverse Optimal Control by introducing projections on singularity curves

Jessica Colombel, David Daney, François Charpillet

***Abstract*— Inverse optimal control (IOC) is a framework used in many fields, especially in robotics and human motion analysis. In this context, various methods of resolution have been proposed in the literature. This article presents Projected Inverse Optimal Control (PIOC), an approach that offers a simple and comprehensive view of IOC methods. Especially, we explain how uncertainties can be properly addressed in our view. Thus, this article highlights how classical methods can be understood as projections of trajectories in the solution space of the underlying Direct Optimal Control (DOC) problem. This perspective allows for an examination of projections other than the classical methods, which can be fruitful for researchers in the field. As an example, we propose a projection that allows us to choose the underlying cost functions of an IOC problem from a set. The IOC's sub-problems are also addressed, such as modelling observed trajectories, noise measurement and the reliability of solutions obtained by IOC. Our proposal is supported by a simple and canonical example throughout the document.**

Inverse Optimal Control, Human Motion Analysis, Identification.

I. Introduction

The Inverse Optimal Control (IOC) is a complex problem studied in many disciplines. We are particularly interested in IOC in the context of human motion analysis. However, the issues go beyond that, in particular, the IOC is related to the Inverse Reinforcement Learning problem whose expression and proposed resolution methods differ [1].

Thanks to this method, the literature analyzes the movement in order to imitate it with a robot [2], [3], to predict human movements to better interact with humans [4], [5] or even to split the movement into sub-tasks [6]. Two methods have been particularly used in the literature: the Bilevel method [2], [7] and the AIOC (Approximately Inverse Optimal Control) method [8], [9]. In the context of human motion analysis, we are particularly interested in IOC under uncertainties: noisy data, uncertain model, unknown cost functions and parameter selection.

This paper proposes an approach that push a comprehensive understanding of IOC methods with respect to uncertainty of observed trajectories, choice of objective functions, and computation complexity. We called it Projected Inverse Optimal Control (PIOC) (Sec. III). This approach is divided into three elements, parametrization of the measurements, decoupling of conditions associated with the successful resolution of the problem and the choice of a solution corresponding to different methods of resolution. Our approach brings a simple and complete view of IOC resolution problem. In particular, we show that the resolutions methods proposed in the literature are equivalent to particular projections in the trajectory space.

Thus, the originality of this paper lies in a new simple view of the IOC problem through:

- parametrization of measurement states and its impact on dimensionality and identifiability of the problem;
- decoupling of conditions: identifiability, singularity and feasibility conditions;
- illustration of the choice of solution by a projection;
- solution for the choice of basis.

First, this paper introduces the problem statement of IOC (Sec. II) by defining Direct Optimal Control (DOC) and Bilevel and AIOC resolution methods. Then, the PIOC approach is presented by detailing its different steps (Sec. III): parametrization, decoupling conditions and choice of solution. We also provide a simple example to illustrate our approach. Finally, we will discuss the perspectives and limitations of the proposed (Sec. IV) approach before concluding this paper (Sec. V).

II. Problem statement

Analysis of human movement by IOC is based on the assumption that human movement is optimal according to a criterion. Bipedal walking is considered as an optimal movement [10], as well as simpler movements such as picking where the hand is following a trajectory minimizing the criterion of torque variation [11]. Moreover, the biological sensorimotor control would itself be governed by optimal laws [12]. Given the multiplicity of movements and their representation, many criteria have been proposed to generate or analyze through IOC human movement [6], [8], [13]–[18]. These cost functions are the basis for the expression of DOC, that generates optimal trajectories.

Following subsections will present the DOC as well as two methods for solving the IOC problem. We will simplify their presentation as much as possible in order to stay pedagogical. Finally, we will discuss limitations of these methods.

A. Direct Optimal Control

In the context of human (or robot) motion, the aim of the DOC is to generate an optimal trajectory $\mathbf{s}^*$ with respect to a given objective or cost function which is considered here to be a weighted sum of elementary cost functions $C(\mathbf{s}) = \sum_{k=1}^{n_c} \omega_k.C_k$, with n_c number of cost functions and with a weight vector $\boldsymbol{\omega} = [\omega_1, \ldots, \omega_{n_c}]$, under n_f equality constraints $f_i(\mathbf{s})$ $(i = 1, \ldots, n_f)$ and n_h inequality constraints $h_j(\mathbf{s})$ $(j = 1, \ldots, n_h)$.

$$\begin{aligned} \mathbf{s}^* &= \arg\min_{\mathbf{s}} C(\mathbf{s}) \\ \textbf{s.t. } & f_{1,\ldots,n_f}(\mathbf{s}) = 0,\ h_{1,\ldots,n_h}(\mathbf{s}) \leq 0 \end{aligned} \tag{1}$$

where $\mathbf{s} \in \mathbb{R}^{n_s \times n_t}$ is a trajectory composed of n_t frames; each are defined by a state $\mathbf{s}_t$ of dimension n_s, such that $\mathbf{s} = [\mathbf{s}_1, \ldots, \mathbf{s}_{n_t}]^T$.

The existence of a solution to this problem is assured by the convexity of the basis $C(\mathbf{s})$ [19]. For that, the literature suggests convexed cost functions (e.g., quadratic) and positive weights $\boldsymbol{\omega}$ [8].

B. Inverse Optimal Control

IOC consists in identifying the basis $C(\mathbf{s})$ that could generate a given (or observed) trajectory $\mathbf{s}_M$ through Eq. 1. This can only be achieved under the assumptions that the cost functions C_k and constraints are known, including the biomechanical kinematic or dynamic model. Thus, the problem is to identify weights $\boldsymbol{\omega}_k$ associated to cost functions C_k. One issue is that the observed trajectory has to be optimal to get a solution to the IOC problem. Fortunately, a lot of resolution methods were proposed to address this issue ([2], [3], [15], [16], [20]). In this paper, we will focus on the two most popular: Bilevel resolution method [2] and Approximate IOC method [8].

1) Bilevel IOC: In the context of human motion analysis [2], [14], [21], Bilevel IOC minimizes (upper-level) the distance of an observed trajectory $\mathbf{s_M} \in \mathbb{R}^{n_s \times n_t}$ to a generated trajectory $\mathbf{s}^*$ by a DOC (lower-level). It forms a bilevel loop which has to converge [22]. Bilevel IOC is expressed as follows:

$$\begin{aligned} &\min_{\boldsymbol{\omega}} \quad \|\mathbf{s}^* - \mathbf{s}_M\|^2 \\ &\textbf{with } \mathbf{s}^* = \underset{\mathbf{s}}{\operatorname{argmin}} \sum_{k=1}^{n_c} \omega_k \sum_{t=1}^{n_t} C_k(\mathbf{s}_t) \\ &\qquad \textbf{s.t. } f_{1,\ldots,n_f}(\mathbf{s}) = 0,\ h_{1,\ldots,n_h}(\mathbf{s}) \leq 0 \end{aligned} \tag{2}$$

If this method is intended to find the weights $\boldsymbol{\omega}$, it should be noted that in this expression, if the observed trajectory $\mathbf{s_M}$ is noisy, the upper-level converges to the optimal trajectory closest to this noisy trajectory.

2) Approximated IOC: Approximate resolution methods are based on verification of optimality conditions associated with Eq. 1. Karush-Kuhn-Tucker (KKT) conditions are largely considered in this framework [6], [9], [13], [23]–[25], although other conditions are possible such as the Jacobi-Bellman equations [26]–[28].

KKT conditions are expressed as follows:

$$\begin{aligned} &\sum_{k=1}^{n_c} \omega_k \frac{\partial C_k}{\partial \mathbf{s}}(\mathbf{s}^*) + \sum_{i=1}^{n_f} \lambda_i \frac{\partial f_i}{\partial \mathbf{s}}(\mathbf{s}^*) \\ &\qquad + \sum_{j=1}^{n_h} \nu_j \frac{\partial h_j}{\partial \mathbf{s}}(\mathbf{s}^*) = \mathbf{0} \quad \text{stationary} \\ &\left.\begin{array}{rl} f_i(\mathbf{s}^*) = 0, & i = 1, \ldots, n_f \\ h_j(\mathbf{s}^*) \leq 0, & j = 1, \ldots, n_h \end{array}\right\} \text{primal feasibility} \\ &\nu_j \geq 0, \quad j = 1, \ldots, n_h \quad \text{dual feasibility} \\ &\nu_j h_j(\mathbf{s}^*) = 0, \quad j = 1, \ldots, n_h \quad \text{complementary slackness} \end{aligned} \tag{3}$$

and the stationary condition can be re-written as:

$$\underbrace{[\mathbf{J}_{\boldsymbol{\omega}}, \mathbf{J}_{\boldsymbol{\lambda}}, \mathbf{J}_{\boldsymbol{\nu}}]}_{\mathbf{J}} \underbrace{\begin{pmatrix} \boldsymbol{\omega} \\ \boldsymbol{\lambda} \\ \boldsymbol{\nu} \end{pmatrix}}_{\mathbf{z}} = \mathbf{0} \tag{4}$$

with $\mathbf{J}$ Identification Matrix and $\mathbf{J}_{\boldsymbol{\omega}}$, $\mathbf{J}_{\boldsymbol{\lambda}}$ and $\mathbf{J}_{\boldsymbol{\nu}}$ sub-matrices associated with the parameters $\boldsymbol{\omega}$ (what the IOC wants to retrieve) and $\boldsymbol{\lambda}, \boldsymbol{\nu}$ unknown Lagrangian coefficients of the constraints of equality and inequality, respectively.

The basis C is convex, so that these conditions are considered necessary but also sufficient for the optimality of the problem [29].

In the literature, these conditions are used to solve the IOC problem by minimizing the residuals through the norm of Eq. 4, see [6], [9], [13], [23].

C. Difficulties of the methods

Each of these methods has limitations that can degrade the analysis of human motion. The main drawback of Bilevel is the computation time due to the double optimization loop [28]. AIOC methods pose problems of robustness [30]. In particular, it is necessary to know to what extent one can trust the results obtained [31].

Moreover, human motion capture is "corrupted" in some way by uncertainty inherent to the sensors that are used for that. This entails that the observed trajectory is deformed making it too far from optimal trajectories that define the solution space of the underlying optimal control problem. Even small distortion makes the problem of IOC unsound. In section II-B we have presented two possible responses to this problem: (1) either IOC is solved as a two level optimisation process in which at the top level the optimal trajectory $\mathbf{s}^*$ is chosen to be as close as possible to the observed trajectory $\mathbf{s}_M$ (Bilevel approach) (2) or it is solved thanks to an approximation in residual approaches. But this issue of uncertainties is not really identified as a major issue in the referred literature. Our view is to better characterize this issue by deepening the strategies taken either in the Bilevel approach or AIOC ones in a unified view. This is why we will develop the notion of trajectory projection from the observation space to the solution space as a way to better understand this issue.

III. Projected Inverse Optimal Control Approach

This section presents our view of IOC. Throughout the article, we illustrate the different notions of our PIOC approach from a simple example already used in literature [20]. Then, we show how to reduce dimensions of the problem to make the approach more robust. After having verified the different feasibility conditions, we show that the IOC problem in the presence of uncertainty amounts to a projection of the observed trajectories on a trajectory belonging to the solution space of the DOC problem given the basis. This view allows to better understand how to choose cost functions and the associated open problems.

A. Canonical example

We propose the same example in our previous article were detailed equations are given [31]: a planar two bar arm with two degrees of freedom θ_1 and θ_2. Both DOC and IOC will be modeled from $n_c = 2$ cost functions of torques: $C = \left\{\tau_1^2, \tau_2^2\right\}$. For each degree of freedom, the state is represented by the angle, its velocity and its acceleration. There is no inequality constraint in this example. Starting and ending point are defined with $\mathbf{s}_1 = [0, 0, 0, 0, 0, 0]$ and $\mathbf{s}_{n_t} = [120, 40, 0, 0, 0, 0]$, respectively.

B. Parametrization: reduction of the dimension

DOC and IOC are processes which are looking for a needle (optimal trajectories) in a haystack (set of admissible trajectories of the considered dynamic system). But, state trajectories are defined in a continuous hyperspace and they can only be observed through sensors that produce samples that are unfortunately corrupted by measurement errors. This raises up several issues that we will be addressed in this section, such as parametrization and reconstruction of state trajectories.

In many contributions to human motion analysis, state variables are typically the joint variables $(q_k, \dot{q}_k, \ddot{q}_k)$ for each observation k. For instance, in our example of previous subsection III-A, if we measure the 2 joints and their derivatives $(\theta_{1,2}, \dot{\theta}_{1,2}, \ddot{\theta}_{1,2})$ during 30s at 25Hz, we observe a vector ($\dim n_s = 3 \times 2 = 6$) on $n_t = 30 \times 25 = 750$ points: the number of state variables is then $n_s * n_t = 4500$.

This large number of variables decrease the robustness and stability of solvers and increase the computation time. In order to tackle the problem, we propose to simplify the modeling of our trajectories by a polynomial representation. This is considered in the literature to represent human motion [32], [33], and even for IOC [6], [23] to model the observed trajectory $\mathbf{s}_M$. However, this is essentially used to filter the measurement noise through a degree-limited polynomial representation which is then re-segmented to discretize the problem. We propose to keep the polynomial representation for $\mathbf{s}$ throughout the modeling and optimization process of IOC. Thus the state variables become the coefficients of the polynomial. This solution allows to drastically reduce the number of variables but limits the dimension of the trajectory representation space which can be seen as an approximation of its real space. In the case of human motion analysis, this allows to limit the influence of noise and to make our results more robust. Nevertheless, the limits on the maximum value of the degree of polynomial remain to be discussed. In our case, one of the interests of this representation is that it allows to consider the trajectories and their derivatives in the same simple formalization. Thus, the equations that link the joint variables and their derivatives to model the dynamics of the system disappear, further reducing the number of constraints and then variables. Please note that the choice of the degree of the polynomial to represent a trajectory and its dynamics is not a trivial matter and several remarks are made on this subject later.

A second simplification is to limit the representation space by considering the starting point $t = 0$ and ending point $t = 1$ of the trajectory which are generally provided. Other intermediate points could be used, again at the expense of reducing the representation space.

Let $Q(t), \dot{Q}(t), \ddot{Q}(t)$ be a polynomial and its derivatives describing the trajectory of a state parameter q, such that $Q(t) = \sum_{k=0}^{n_d} \alpha_k\, t^k$, $\dot{Q}(t) = \sum_{k=1}^{n_d} k\, \alpha_k\, t^{k-1}$, $\ddot{Q}(t) = \sum_{k=2}^{n_d} k\,(k-1)\, \alpha_k\, t^{k-2}$, with n_d the degree of the polynomial.

At the starting (resp. ending) point $t = 0$ (resp. $t = 1$), $Q(0) = q_0, \dot{Q}(0) = \dot{q}_0, \ddot{Q}(0) = \ddot{q}_0$ (resp. $Q(1) = q_1, \dot{Q}(1) = \dot{q}_1, \ddot{Q}(1) = \ddot{q}_1$) with $(q_0, \dot{q}_0, \ddot{q}_0)$ (resp. $(q_1, \dot{q}_1, \ddot{q}_1)$) the position, velocity and acceleration of the starting (resp. ending) of the variable q of the observed trajectory $\mathbf{s_M}$. This forms a system of 6 linear equations in unknowns α_k, $k = 0, \ldots, n_d$. If $n_d > 5$, this linear system allows to determine a subpart ($\dim = n_d - 5$) of α_k in function of the others, in other words to eliminate parts of α_k. The dimension which models all possible polynomials trajectories from $(q_0, \dot{q}_0, \ddot{q}_0)$ to $(q_1, \dot{q}_1, \ddot{q}_1)$ is equal to $n_d - 5$.

We apply this on example of section III-A by fixing $n_d = 6$: this choice is mainly conducted to provide a simple 2D graphical interpretation of approach. The linear equations, given by the starting and ending points, allow to determine $\alpha_0, \ldots, \alpha_5$ as a function of α_6.

We can then express the polynomial Q only in terms of α_6, as follows:

$$Q(t) = a + b\,t + c\,t^2 + (d - \alpha_6)\,t^3 + (e + 3\,\alpha_6)\,t^4 + (f - 3\,\alpha_6)\,t^5 + \alpha_6\,t^6 \quad (5)$$

with a, b, c, d, e and f scalars only depending on the starting and ending points.

Apply to our example, the joint variables θ_1 can be parameterized by a reduced polynomial such that $\theta_1(t) = Q(t, \alpha_6)$. In the same way a new polynomial in $\beta_{0..6}$ coefficients can describe the second joint variable $\theta_2(t)$ such that $\theta_2(t) = Q(t, \beta_6)$. Then we reduce the variable space from 4500 (see beginning of the paragraph) to two variables α_6, β_6 which can be used to parameterize an IOC.

Remark: If $n_d = 5$, there is only one trajectory that passes through the start and end points: it is then not possible to find in this zero-space a possible optimal trajectory according to a chosen base $C(\mathbf{s})$. We get then a lower bound on n_d for 2 fixed points defined by 3 components (position, velocity, acceleration). An upper bounds on n_d which increase the dimensions of the search space of $\mathbf{s}$ is more difficult to determine because it is not mathematically constrained. However, we know that a polynomial interpolation of too large degree will tend to overfit the experimental data. Complementary, additional constraints on the degree of the polynomial are provided in the next section, especially to consider the number of cost functions C_k but also the number of constraints.

C. Decoupling of conditions

As already introduced in our previous paper [31], the solution of the problem is based on the verification of different conditions derived from KKT. We decouple them in:

- Identifiability conditions;
- Singularity condition;
- Feasibility conditions.

1) Identifiability conditions: For the IOC to admit a solution, all parameters must be identifiable. As detailed in our previous paper [31], submatrices $(\mathbf{J}_\omega, \mathbf{J}_\lambda, \mathbf{J}_\nu)$ associated with parameters need to be full ranks. If not a QR decomposition is suggested to eliminate the superfluous parameters.

Dimensionality: The identifiability is also dependent on the dimensions of the problem. In particular, the problem must have more (or at least equal) parameters than equations (cost functions and constraints). Note that in the context of our parametric approach, the number of rows of $\mathbf{J}$ have to be greater than the number of columns $(\dim(\mathbf{J}) = (n_d - 5) * n_q \times n_c + n_f + n_h)$.

This means that for a given problem, the degree of the polynomial is also affected by the number of constraints (n_f, n_h) but also by the number of cost function n_c chosen for C. This underlines the importance of adapting the dimension of the space of the state variables to the considered basis C and thus to increase the degree in function.

For example with our illustration III-A, where $n_h = 0$ and $n_f = 0$, we fix the polynomials degree to 6 ($n_d = 6$). Then, as mentioned before, the state variables are α_6 and β_6: the matrix $\mathbf{J}$ obtained is of size 2×2. If we want to study $n_c = 4$ cost functions C_k, we must increase the degree of the polynomial to $n_d = 7$. Thus, this constraints the lower bound on n_d.

2) Singularity condition: The KKT stationary condition is a necessary but not sufficient condition to express the optimality of the trajectory. This means the Identification Matrix $\mathbf{J}$ needs to be singular to admit a non-trivial solution. However, we need an analytical expression of this condition that should be expressed as: $det(\mathbf{J}^T\mathbf{J}) = 0$ ($\mathbf{J}$ is not necessary square).

With our example, it is possible to display this condition, $det(\mathbf{J}^T\mathbf{J}) = 0$, in the trajectory space parametrized by α_6 and β_6. We call the curve obtained the "singularity curve" (Fig. 1) and a zoom on a portion (red square) on which all the trajectories from the DOC are.

We can remark that :

- all points in the plane describe a possible trajectory connecting the starting and ending points including the observed trajectory $\mathbf{s}_M$;
- we can give a values for $\boldsymbol{\omega}$ (not necessary positive) for each point of the plane by computing the singular vector associated with the smallest singular value of $\mathbf{J}$ (see SVD resolution in [31]).
- only white points realize the KKT stationary condition given for a chosen basis C and can be a candidate for $\mathbf{s}^*$.

3) Feasibility conditions: In our approach, we distinguish two types of feasibility conditions: those of KKT feasibility and the one on the convexity of the problem. The primal feasibility conditions associated with the constraints may not be respected exactly in a context of uncertainty. This point is discussed in [31]. To realize the condition associated to the convexity of $C(\mathbf{s})$ (sec. II-A): the weights ω_k have to be positive. Therefore, only the points on the singularity curve for which we can associate positive weights can be candidate for $\mathbf{s}^*$. We prefer to conserve this as a condition and do not consider it as a constraint as in [6], [23], [24]. We consider that the constraint forces the $\boldsymbol{\omega}$ to be positive and thus modify the result to fit it, even if it means a huge deviation from the observed trajectory. Using it as a condition allows us to invalidate the result if the weights are negative.

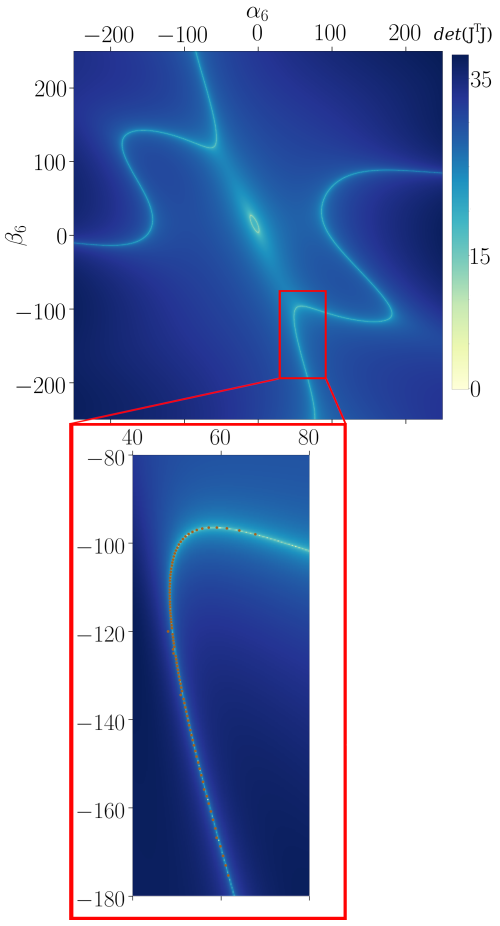

Fig. 1: Illustration of a singularity curve ($det(\mathbf{J}^T\mathbf{J}) = 0$) from the example in section III-A. Two axes represents the free parameters α_6 and β_6 which parameterize the angle θ_1 and θ_2, respectively. The color map is the value of $det(\mathbf{J}(\alpha_6, \beta_6)^T\mathbf{J}(\alpha_6, \beta_6))$.

D. Choice of solution: projection

The previous sections have shown how to reduce the search space of trajectories in such a way optimal one $\mathbf{s}^*$ can be efficiently found. Thus, the parts of the singularity curve for which one can associate positive ω can contain potential solutions for $\mathbf{s}^*$. Their computation depends only on the starting and ending points and on the choice of a cost function C_k, parametrized by the coefficients of polynomials modeling a trajectory in a generic way. Ideally, i.e., without measurement error, for the exact choice of DOC generator cost functions, the observed curve $\mathbf{s}_M$ must lie on the feasible parts of the singularity curve. The weights ω_k are then simply computed by means of an SVD.

However, the errors in the measurements resulting from the observation of the trajectory displace it from its ideal. The first issue is to understand how to project $\mathbf{s}_M$ on the singularity curve to obtain $\mathbf{s}^*$. We will see that this corresponds to the

different approaches of the domain.

The second issue is to answer the question of the validity of the cost functions C_k chosen by hypothesis. We will show that our view can bring some answers.

1) Type of projection: In this paper, we have mentioned two methods used in the literature for the application of IOC to human motion analysis: Bilevel and AIOC (Sec. II-B). These methods of solving the IOC problem correspond, for us, to different projections, one orthogonal and the other one that we will call "iso-weighted". Figure 2 illustrates these two projections for two uncertain trajectories.

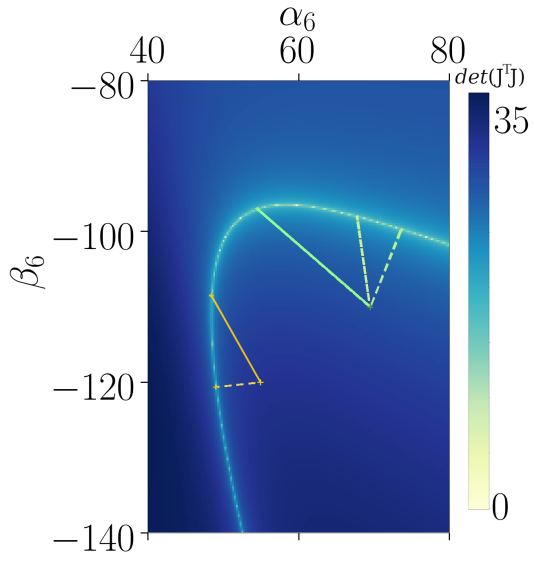

Fig. 2: Comparison of projections for two trajectories in green and yellow on a singularity curve graph (Fig. 1). For each trajectory, the projection in plain line is iso-weighting and the dotted lines are "orthogonal". Note that the green trajectory has two dotted projections, one has weight constraints ($\boldsymbol{\omega} \geq 0$) which distorts the projection, the other has no constraints and is indeed orthogonal.

a) Iso-weighted projection: The iso-weighted projection is obtained with the resolution of an unconstrained AIOC on $\boldsymbol{\omega}$. The resolution of AIOC corresponds the computation of $\boldsymbol{\omega}$ though a Singular Value Decomposition of the matrix $\mathbf{J}(\mathbf{s}_M)$ evaluate in $\mathbf{s}_M$ - see [31]. However, if we use this solution $\boldsymbol{\omega}^\star$ in a DOC, we obtain a trajectory $\mathbf{s}^\star$ on the singularity curve. In fact, the DOC converge to a minimum of C along a path composed by points for which $\boldsymbol{\omega}$ are constant. This coincides to the curve (near of a line), see Figure 2 linking the point $\mathbf{s}_M$ and $\mathbf{s}^\star$: all the points have the same value of $\boldsymbol{\omega}$. It is why we call it an iso-weighted projection. Figure 3 shows for each trajectory, which weight $\boldsymbol{\omega}$ is associated. In our example, $\boldsymbol{\omega}$ is a vector of size $n_c = 2$, so it is possible to express this vector as an angle ($\|\boldsymbol{\omega}\| = 1$). Both yellow/red areas are for the positive values of $\boldsymbol{\omega}$. A color represents a fixed value of $\boldsymbol{\omega}$. Therefore, they represent the areas in which it is possible to obtain a solution to the IOC problem with this resolution method.

b) Orthogonal Projection: We have identified through the singularity curves a set of optimal trajectories associated to

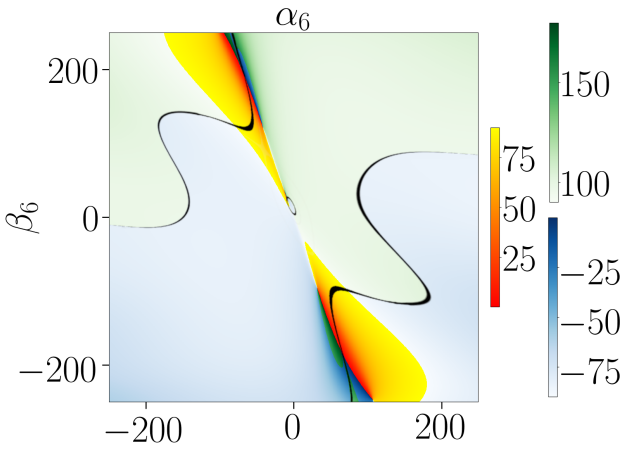

Fig. 3: Illustration of the iso-weighted area. Two axis are the free parameters α_6 and β_6 from the angle θ_1 and θ_2, respectively. The black curve is the singularity curve associated to the example basis C. The colormap shows the angle (in degree) that represents the vector $\boldsymbol{\omega}$ of size 2. In yellow/red, $\boldsymbol{\omega}$ is positive.

cost functions C_k given by $det(\mathbf{J}(\mathbf{s})^T\mathbf{J}(\mathbf{s}) = 0$. The natural proposal is therefore simply to project orthogonally on this space the observed trajectory $\mathbf{s}_M$ as :

$$\begin{aligned} \mathbf{s}^* = \arg\min_{\mathbf{s}} \quad & \|\mathbf{s} - \mathbf{s}_M\|^2 \\ \textbf{s.t. } & det(\mathbf{J}(\mathbf{s})^T\mathbf{J}(\mathbf{s})) \quad = 0 \end{aligned} \tag{6}$$

This can be easily done because the distance between two trajectories parametrized by polynomials is proportional to the distance of the state variable given by the free coefficients. Let ξ_p be the path error between two polynomials $Q(t)$ et $Q'(t)$, according to the equation (Eq. 5) such that:

$$\begin{aligned} \xi_p &= \int_0^1 (Q(t) - Q'(t))\,\mathrm{d}t \\ &= \Delta_\alpha \int_0^1 (-t^3 + 3\,t^4 - 3\,t^5 + t^6)\,\mathrm{d}t = -\frac{\Delta_\alpha}{140} \end{aligned} \tag{7}$$

with $\Delta_\alpha = \alpha_6 - \alpha_6'$. The same reasoning can be applied to each observed state as well as with a higher polynomial degree. Then, the distance between two states (here parameterized by α_6, β_6) is proportional to the distance between two trajectories. Now, in the space of parametric trajectories, the minimum squared norm is the shortest distance, which corresponds to an orthogonal projection between the measured trajectory parameters and those of the trajectories on the singularity curves.

We can remark that the resolution of the IOC problem with a Bilevel is also an orthogonal projection in regards to upper-level. The lower-level, based on a DOC, guarantees the convexity of the basis. Thus, since the low level is a DOC, $\boldsymbol{\omega}$ are necessarily positive. Choosing the solution corresponding to a Bilevel then consists in taking the optimal trajectory closest to the observed trajectory. In other words, an orthogonal projection constrained by positive omega.

As we said before, it does not seem relevant to us to constrain the positivity of $\boldsymbol{\omega}$ but rather to use it as a condition

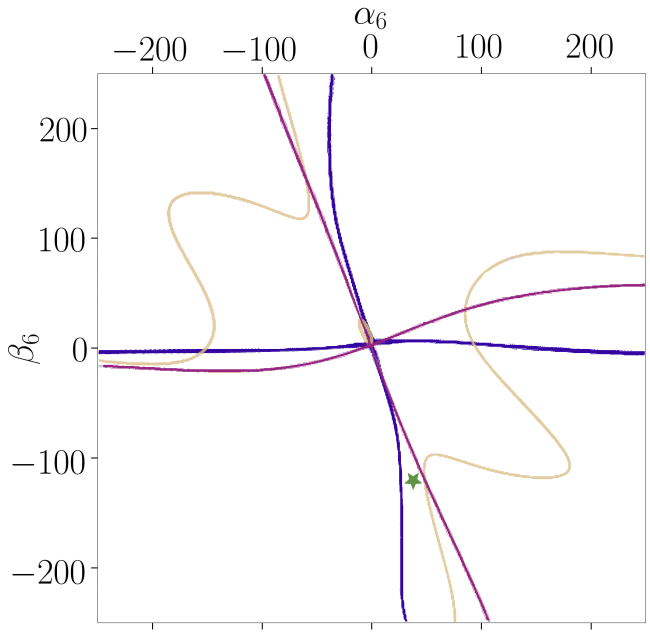

Fig. 4: Illustration of 3 singular curves: $C = [\tau_1, \tau_2]$ (yellow), $C' = [\dot{\theta}_1\,\tau_1, \dot{\theta}_2\,\tau_2]$ (blue) and $C'' = [\ddot{\theta}_1\,\tau_1, \ddot{\theta}_2\,\tau_2]$ (purple). The green point corresponds to a uncertain trajectory. It is not obvious which cost function basis to choose in this configuration.

(Sec III-C). This choice of projection which would be purely orthogonal would correspond to a method also used in the literature: the Onelevel IOC [34]. This method is composed by the high level of the bilevel but under KKT condition constraints. Equation 6 is a simpler approach of the Onelevel because we use the determinant rather than all the KKT conditions. It brings the advantage of decoupling the feasibility problem from the resolution, which is at the heart of our approach.

2) Choice of basis: The approach proposed in this paper aims to address many problems of IOC resolution in the context of human movement. The choice of the cost functions used to generate the observed trajectory is one of them. Figure 4 shows three singularity curves corresponding to three different sets of $C_k^{'}, C_k^{''}, C_k^{'''}$ respectively to torque, angular power and acceleration multiplied by torque. If we observe a trajectory in the middle of its curves, how can we choose the best basis?

A simple way to select the basis is then to choose as function of the distance in state space between observed trajectory $\mathbf{s}_M$ and these projection on each basis (without solving the problems of ambiguity raised in Figure 4). A backdraft of this approach is the computation time needed to check a large number of possible combination of cost functions. An other solutions is to compute the distance through the evaluation of the different determinants of each basis as $\det(\mathbf{J}_{C_k^{'}}(\mathbf{s}_M)), \det(\mathbf{J}_{C_k^{''}}(\mathbf{s}_M)), \det(\mathbf{J}_{C_k^{'''}}(\mathbf{s}_M)), \ldots$. This raises the question of the normalization of matrices $\mathbf{J}$ calculated for different basis $C_k^{'}$...to obtain the same variations of their determinants as a function of same state variable variations. This point is important to start to consider directly the uncertainties modelling in our algorithms.

IV. Discussion and perspectives

In the presence of uncertainty, the IOC problem can be view as the construction of a representation of a set of optimal trajectories with regard to a basis, and then to identify the one, among this set, that can correspond to an observation of a real world trajectory.

From this proposal, we can build perspectives on many points of the approach:

- The construction of singular trajectory sets depends on their representation but also on the chosen optimality criteria. We use the KKT conditions, however the same approach can be taken with the Jacobi-Bellman conditions [26].
- In the same way, the polynomial representation is not the only possibility that we have at our disposal to simplify the representation and especially to reduce the dimensions of the problem.
- The integration in our model of uncertainty should allow us to identify metrics to qualify the solution of the IOC.
- If two types of projections are listed in this paper, others can also emerge. Note that in the case of human motion analysis, the orthogonal projection is the more natural.
- Finally, the notion of projection on an ideal of observed trajectories opens possibilities of algorithms for the selection of cost functions.

Thus, our approach opens up many elements. Each of the steps proposed in PIOC can be transposed with other methods.

It should also be noted that, if the work presented is motivated by the analysis of human movement, the proposed method is adapted to many other applications.

V. Conclusion

This article presents an approach called PIOC which we have qualified as holistic in the sense that it presents under a unified view a certain number of difficult questions treated in a singular way by different approaches as proposed by the robotic community. The notion of projection of trajectories into the space of optimal trajectories allows us to bring together algorithms that were previously differently studied, such as the Bilevel IOC and AIOC. This view, although it may seem trivial, is nonetheless extremely fruitful for moving forward. Indeed, it clearly lays the foundations for developing a framework working in the wild, mixing data-driven and model-based approaches. We can thus benefit from two worlds going from Machine Learning for (1) trajectory representation and classical (2) control theory. Concerning (1) we only have introduced the topic using polynomial representation, but we keep in mind other approaches we did not developed here for the sake of simplicity. But approaches such as ProMP or deep learning are good candidates for going forward.

REFERENCES

[1] N. Ab Azar, A. Shahmansoorian, and M. Davoudi, "From inverse optimal control to inverse reinforcement learning: A historical review," *Annual Reviews in Control*, vol. 50, pp. 119–138, Jan. 2020.

[2] K. Mombaur, A. Truong, and J.-P. Laumond, "From human to humanoid locomotion—an inverse optimal control approach," *Autonomous Robots*, vol. 28, no. 3, pp. 369–383, Apr. 2010.

[3] T. Park and S. Levine, "Inverse Optimal Control for Humanoid Locomotion," p. 5, 2013.

[4] J. Mainprice, R. Hayne, and D. Berenson, "Predicting human reaching motion in collaborative tasks using Inverse Optimal Control and iterative re-planning," in *2015 IEEE International Conference on Robotics and Automation (ICRA)*, May 2015, pp. 885–892.

[5] S. Gaurav and B. Ziebart, "Discriminatively Learning Inverse Optimal Control Models for Predicting Human Intentions," in *Proceedings of the 18th International Conference on Autonomous Agents and MultiAgent Systems*, ser. AAMAS '19. Montreal QC, Canada: International Foundation for Autonomous Agents and Multiagent Systems, May 2019, pp. 1368–1376.

[6] J. F.-S. Lin, V. Bonnet, A. M. Panchea, N. Ramdani, G. Venture, and D. Kulić, "Human motion segmentation using cost weights recovered from inverse optimal control," in *2016 IEEE-RAS 16th International Conference on Humanoid Robots (Humanoids)*, Nov. 2016, pp. 1107–1113.

[7] S. Albrecht, P. Basili, S. Glasauer, M. Leibold, and M. Ulbrich, "Modeling and Analysis of Human Navigation with Crossing Interferer Using Inverse Optimal Control," *IFAC Proceedings Volumes*, vol. 45, no. 2, pp. 475–480, Jan. 2012.

[8] A. Panchea, *Inverse Optimal Control for Redundant Systems of Biological Motion*. Orléans, Dec. 2015.

[9] A.-S. Puydupin-Jamin, M. Johnson, and T. Bretl, "A convex approach to inverse optimal control and its application to modeling human locomotion," in *2012 IEEE International Conference on Robotics and Automation*, May 2012, pp. 531–536.

[10] R. M. Alexander, "The Gaits of Bipedal and Quadrupedal Animals," *The International Journal of Robotics Research*, vol. 3, no. 2, pp. 49–59, Jun. 1984.

[11] Y. Uno, M. Kawato, and R. Suzuki, "Formation and control of optimal trajectory in human multijoint arm movement," *Biological Cybernetics*, vol. 61, no. 2, pp. 89–101, Jun. 1989.

[12] E. Todorov, "Optimality principles in sensorimotor control," *Nature Neuroscience*, vol. 7, no. 9, pp. 907–915, Sep. 2004.

[13] P. Carreno-Medrano, T. Harada, J. F.-S. Lin, D. Kulić, and G. Venture, "Analysis of Affective Human Motion During Functional Task Performance: An Inverse Optimal Control Approach," in *2019 IEEE-RAS 19th International Conference on Humanoid Robots (Humanoids)*, Oct. 2019, pp. 461–468.

[14] D. Clever, R. Malin Schemschat, M. L. Felis, and K. Mombaur, "Inverse optimal control based identification of optimality criteria in whole-body human walking on level ground," in *2016 6th IEEE International Conference on Biomedical Robotics and Biomechatronics (BioRob)*, Jun. 2016, pp. 1192–1199.

[15] D. Clever and K. Mombaur, "An Inverse Optimal Control Approach for the Transfer of Human Walking Motions in Constrained Environment to Humanoid Robots," in *Robotics: Science and Systems XII*. Robotics: Science and Systems Foundation, 2016.

[16] B. Berret, E. Chiovetto, F. Nori, and T. Pozzo, "Evidence for Composite Cost Functions in Arm Movement Planning: An Inverse Optimal Control Approach," *PLOS Computational Biology*, vol. 7, no. 10, p. e1002183, Oct. 2011.

[17] K. Mombaur, A.-H. Olivier, and A. Crétual, "Forward and Inverse Optimal Control of Bipedal Running," in *Modeling, Simulation and Optimization of Bipedal Walking*, ser. Cognitive Systems Monographs, K. Mombaur and K. Berns, Eds. Berlin, Heidelberg: Springer, 2013, pp. 165–179.

[18] J. R. Rebula, S. Schaal, J. Finley, and L. Righetti, "A Robustness Analysis of Inverse Optimal Control of Bipedal Walking," *IEEE Robotics and Automation Letters*, vol. 4, no. 4, pp. 4531–4538, Oct. 2019.

[19] S. P. Boyd and L. Vandenberghe, *Convex Optimization*. Cambridge, UK ; New York: Cambridge University Press, 2004.

[20] W. Jin, D. Kulić, S. Mou, and S. Hirche, "Inverse Optimal Control with Incomplete Observations," *arXiv:1803.07696 [cs]*, May 2019.

[21] S. Albrecht, M. Ulbrich, and M. Leibold, "A bilevel optimization approach to obtain optimal cost functions for human arm movements," *Numerical Algebra, Control and Optimization*, vol. 2, no. 1, pp. 105–127, Mar. 2012.

[22] A. Sinha, P. Malo, and K. Deb, "A Review on Bilevel Optimization: From Classical to Evolutionary Approaches and Applications," *IEEE Transactions on Evolutionary Computation*, vol. 22, no. 2, pp. 276–295, Apr. 2018.

[23] A. M. Panchea and N. Ramdani, "Towards solving inverse optimal control in a bounded-error framework," in *2015 American Control Conference (ACC)*, Jul. 2015, pp. 4910–4915.

[24] P. Englert, N. A. Vien, and M. Toussaint, "Inverse KKT: Learning cost functions of manipulation tasks from demonstrations," *The International Journal of Robotics Research*, vol. 36, no. 13-14, pp. 1474–1488, Dec. 2017.

[25] N. Aghasadeghi and T. Bretl, "Inverse optimal control for differentially flat systems with application to locomotion modeling," in *2014 IEEE International Conference on Robotics and Automation (ICRA)*, May 2014, pp. 6018–6025.

[26] E. Pauwels, D. Henrion, and J.-B. Lasserre, "Inverse optimal control with polynomial optimization," in *53rd IEEE Conference on Decision and Control*, Dec. 2014, pp. 5581–5586.

[27] T. L. Molloy, J. J. Ford, and T. Perez, "Finite-horizon inverse optimal control for discrete-time nonlinear systems," *Automatica*, vol. 87, pp. 442–446, Jan. 2018.

[28] M. Johnson, N. Aghasadeghi, and T. Bretl, "Inverse optimal control for deterministic continuous-time nonlinear systems," in *52nd IEEE Conference on Decision and Control*, Dec. 2013, pp. 2906–2913.

[29] M. A. Hanson, "On sufficiency of the Kuhn-Tucker conditions," *Journal of Mathematical Analysis and Applications*, vol. 80, no. 2, pp. 545–550, Apr. 1981.

[30] A. Aswani, Z.-J. M. Shen, and A. Siddiq, "Inverse Optimization with Noisy Data," *Operations Research*, vol. 66, no. 3, pp. 870–892, Jun. 2018.

[31] J. Colombel, D. Daney, and F. Charpillet, "On the Reliability of Inverse Optimal Control," in *2022 International Conference on Robotics and Automation (ICRA)*, May 2022, pp. 8504–8510.

[32] C. Taylor, B. konskyvon Konsky, and C. Kirtley, "Polynomial approximations of gait for human motion analysis and visualization," in *Proceedings of the 20th Annual International Conference of the IEEE Engineering in Medicine and Biology Society. Vol.20 Biomedical Engineering Towards the Year 2000 and Beyond (Cat. No.98CH36286)*, vol. 5, Nov. 1998, pp. 2490–2493 vol.5.

[33] N. Hogan and D. Sternad, "Sensitivity of Smoothness Measures to Movement Duration, Amplitude, and Arrests," *Journal of Motor Behavior*, vol. 41, no. 6, pp. 529–534, Nov. 2009.

[34] K. Hatz, J. P. Schlöder, and H. G. Bock, "Estimating Parameters in Optimal Control Problems," *SIAM Journal on Scientific Computing*, vol. 34, no. 3, pp. A1707–A1728, Jan. 2012.